

[28] Calorimetry: A Tool for DNA and Ligand–DNA Studies

By KENNETH J. BRESLAUER, ERNESTO FREIRE, and MARTIN STRAUME

Introduction

Calorimetry occupies a venerable place in the history of science. In fact, during the 1700s, 1800s, and 1900s, the nature and measurement of heat has captured the attention of some of the giants of science, including Fahrenheit, Black, Watt, Lavoisier, Carnot, Cavendish, Joules, Kelvin, Clausius, Dalton, Hess, Bunsen, Thomsen, Berthelot, Gibbs, Helmholtz, Curie, and Nernst. Their interest in calorimetry derived, in part, from the belief that the heat change accompanying a reaction could serve as a measure of the affinity of the reacting species for one another, as well as a measure of the spontaneity of the reaction. These beliefs motivated the extensive thermodynamic studies of Thomsen and Berthelot. However, once the contributions of Guldberg, Waage, Gibbs, and Helmholtz made it clear that the spontaneity of a process depended on a decrease in *free energy* rather than *enthalpy*, the field of thermochemistry suffered neglect. A rebirth of interest in thermochemistry occurred at the beginning of the twentieth century when it was shown that enthalpy and heat capacity data could be used to calculate free energies.

As calorimeters are instruments that permit the direct and quantitative measurement of heat, it should not be surprising to learn that many of the giants of science noted above were the first to build calorimeters, thereby establishing the field of calorimetry. For example, in 1760, Black built the first “phase-transition calorimeter” and used it to demonstrate how the heat delivered to melting ice induces a phase transition (from ice to liquid water) rather than a temperature rise, thereby establishing the distinction between temperature and heat. In 1903, Pierre Curie developed a twin Dewar vessel “microcalorimeter” and used it to measure the heat output accompanying the decay of radium bromide.

For the most part, the early calorimeters were used to measure heat changes accompanying simple, well-defined processes (e.g., ice melting and radioactive decay). However, it is of interest to note that some of the earliest calorimetric studies were conducted on more complex “biological” systems. This observation is of particular interest in light of the frequently lamented rift between the two cultures of biology and chemistry.¹ However, a brief review of the history of calorimetry reveals that this current rift cannot be blamed on the past. For example, in 1780, Lavoisier and Laplace built an “ice calorimeter” in which they placed a guinea pig. They

measured the amount of ice melted and CO₂ produced by the animal over a 10-hr period and compared this with the heat produced in 10 hr on combustion of the equivalent amount of carbon. The experiment was inspired by their notion that animal respiration could be equated to simple combustion, so that the heat produced on exhalation of a specific amount of CO₂ should equal the heat produced by oxidation of the corresponding amount of carbon. In some sense, the measurements of Lavoisier and Laplace heralded the beginning of the field of biocalorimetry. Subsequent calorimetric studies on biological systems (including whole organisms) were pursued throughout the early nineteenth and twentieth centuries by scientists such as Dubrunfaut, Tangl, Meyerhof, Voit, Atwater, Bayne-Jones, and others.²⁻⁵ In the aggregate, these studies led to the conclusion that the first law of thermodynamics was valid for living organisms as well as for the inorganic world, thereby placing the field of biocalorimetry on firm ground.

Despite this impressive history, during the first half of the twentieth century the field of biocalorimetry was not widely embraced by the scientific community. However, during the 1960s, 1970s, and 1980s, biocalorimetry has experienced an explosive rebirth. This renewed interest can be attributed to four important factors. First, major advances in electronics have vastly improved the sensitivity of modern calorimetric instrumentation. Second, improvements in synthetic methodologies and biochemical separations/purifications now make available samples of sufficient purity and quantity for calorimetric measurements. Third, the development of theoretical formalisms coupled with advancements in computer technology now makes it possible to extract the maximum amount of information inherent in the raw calorimetric data. Finally, commercialization has made highly sensitive microcalorimeters more generally available to the scientific community so that the field of biocalorimetry no longer is restricted to those laboratories capable of building their own instruments.

The specific purpose of this chapter is to provide the reader with an overview of how calorimetric techniques can be used to study nucleic acid systems, particularly DNA. Consequently, no attempt will be made to present a comprehensive survey of the substantial literature that exists in this area. For such information the reader is referred to books on calorimetry,⁶⁻⁹ previously published reviews,¹⁰⁻¹⁸ as well as the original

¹ A. Kornberg, *Biochemistry* **26**, 6888 (1987).

² M. Debrunfaut, *C. R. Hebd. Séances Acad. Sci.* **42**, 945 (1856).

³ O. Meyerhof, "Chemical Dynamics in Life Phenomena," Monograph, p. 110. 1924.

⁴ S. Bayne-Jones and H. S. Rhee, *J. Bacteriol.* **17**, 123 (1929).

⁵ S. Bayne-Jones, *J. Bacteriol.* **17**, 105 (1929).

⁶ W. Hemminger and G. Höhne, "Calorimetry." Verlag Chemie, Weinheim, Germany, 1984.

⁷ M. N. Jones, ed., "Biochemical Thermodynamics." Elsevier, Amsterdam, 1979.

research articles referenced in these books and review chapters. Instead, this chapter is designed to emphasize the unique information that can be obtained by application of selected calorimetric techniques to the study of DNA. To this end, we have organized the chapter into sections in which the presentation of each calorimetric technique is divided into three parts. The first two parts of each section provide, in nontechnical terms, a brief description of a particular technique followed by an outline of the information content of the method. The third and final part of each section presents one or more examples of how the technique has been used to study DNA. These examples have been selected for illustrative purposes only, and they generally reflect the tastes and prejudices of the authors rather than an assessment of the importance of the work.

Differential Scanning Calorimetry

Method

A differential scanning calorimeter (DSC) is an instrument that allows one to measure continuously the heat capacity of a system as a function of temperature. The technical features of DSC instruments previously have been described in detail^{15,17} (see also references cited in both of these excellent reviews). In general terms, a typical DSC instrument contains two cells which are suspended within adiabatic shields and connected via a multijunction thermopile. Figure 1 shows schematics of such a DSC instrument. The cells are filled through capillary tubes that are accessed via external filling ports. In a typical experiment, the reaction and the reference cell are each filled completely (~1 ml), and the temperature is

⁸ H. D. Brown, ed., "Biochemical Microcalorimetry." Academic Press, New York and London, 1969.

⁹ A. E. Breezer, ed., "Biological Microcalorimetry." Academic Press, New York, 1980.

¹⁰ H.-J. Hinz, in "Biochemical Thermodynamics" (M. N. Jones, ed.), p. 116. Elsevier, Amsterdam, 1979.

¹¹ W. Pfeil, in "Thermodynamic Data for Biochemistry and Biotechnology" (H.-J. Hinz, ed.), p. 349. Springer-Verlag, Berlin, 1986.

¹² K. J. Breslauer, in "Thermodynamic Data for Biochemistry and Biotechnology" (H.-J. Hinz, ed.), p. 402. Springer-Verlag, Berlin, 1986.

¹³ G. Rialdi and R. Biltonen, in "MPT International Review of Science, Physical Chemistry." Medical and Technical Publ., and Butterworth, London, 1975.

¹⁴ J. M. Sturtevant, *Annu. Rev. Biophys. Bioeng.* **3**, 35 (1974).

¹⁵ J. M. Sturtevant, *Annu. Rev.* **38**, 463 (1987).

¹⁶ I. Wadso, in "MPT International Review of Science, Physical Chemistry Series One" (H. A. Skinner, ed.), Vol. 10. Butterworth, London, 1972.

¹⁷ P. L. Privalov and S. A. Potekhin, this series, Vol. 131, p. 4.

¹⁸ P. D. Ross, in "Procedures in Nucleic Acid Research" (G. L. Cantoni and D. R. Davies, eds.), Vol. 2. Harper & Row, New York, 1971.

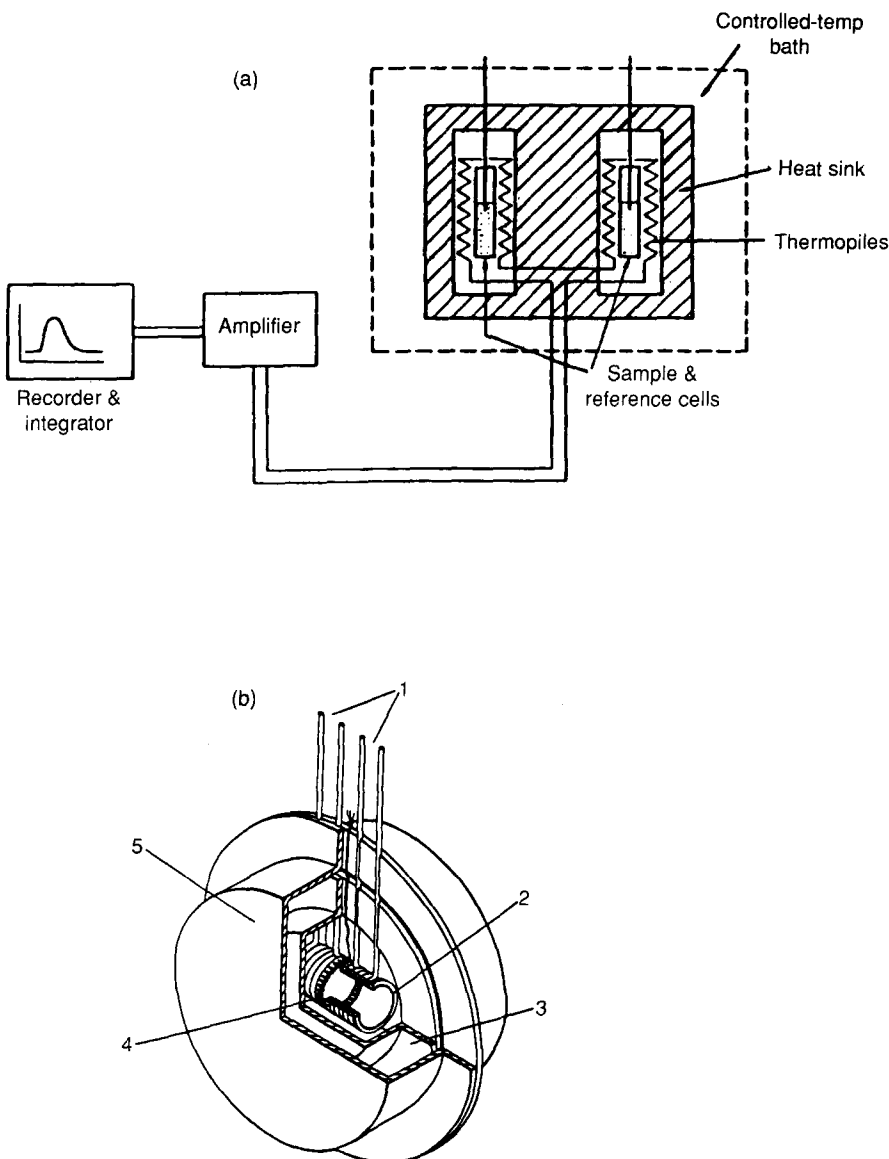


FIG. 1. (a) Schematic of the components of a typical differential scanning calorimeter. (b) Schematic representation of the cells and adiabatic shields of the DASM-4 differential scanning microcalorimeter. 1, Capillary inlets; 2, capillary cell; 3, inner shield; 4, thermopile between the cells; 5, outer shield. (By permission of Pergamon Press, Ltd.)

scanned from about 0 to 100° using electrical heaters which are in good thermal contact with the cells. When a thermally induced endothermic transition occurs in the sample cell, the temperature of this cell will lag behind that of the solvent reference cell, since some of the electrical energy is required to induce the transition rather than to increase the temperature of the solution. This temperature difference between the two cells is sensed by the thermopile and activates a circuit which adds additional electrical energy to the reaction cell so as to maintain it at the same temperature as the solvent reference cell. This compensating electrical energy, which is proportional to the energy associated with the thermally induced transition, is recorded. The instrument is calibrated by measuring the area produced by an electrical pulse of known energy.

These data, along with the known concentration of the solute, permit conversion of the observed electrical energy versus temperature curve to the corresponding C_p^{ex} versus temperature (T) curve, where C_p^{ex} is the excess heat capacity of the DNA solution relative to the reference buffer. A typical heat capacity curve measured for the thermally induced transition of an oligomeric DNA sample is shown in Fig. 2a. It is of interest to note

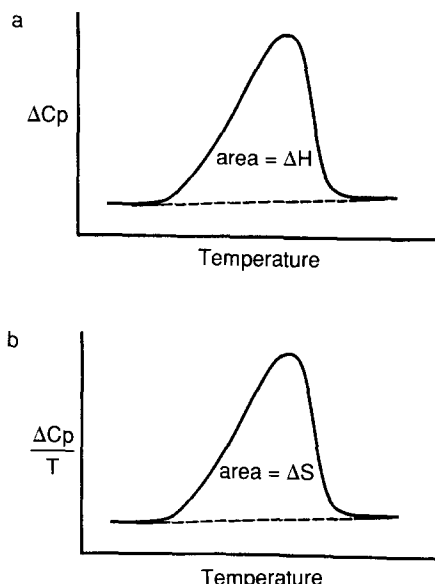


FIG. 2. (a) Typical calorimetric transition curve, which shows how the heat capacity, ΔC_p , changes with temperature. The area under the curve is equal to the transition enthalpy. (b) A $\Delta C_p/T$ versus temperature curve, which can be derived from the experimental calorimetric transition curve shown in (a). The area under the curve is equal to the transition entropy.

that, in most studies, the excess heat capacity at the peak of the transition is less than 1% of the total solution heat capacity. This feature emphasizes the need for DSC instruments of high sensitivity and precision.

Information Content

A single DSC profile provides a wealth of thermodynamic and extrathermodynamic information about a thermally induced DNA transition. Specifically, as described below, from a single heat capacity versus temperature curve, one can derive the following information: the transition free energy (ΔG^0), enthalpy (ΔH^0), entropy (ΔS^0), and heat capacity (ΔC_p); the "stateness" of the transition (two-state versus multistate); the average size of the molecule that melts as a single thermodynamic entity (e.g., the size of the cooperative unit); the cooperativity parameter, σ , as defined in the theoretical formalism of Zimm and Bragg¹⁹ as well as Applequist²⁰; and the partition function for the transition.²¹⁻²³ Knowledge of the partition function allows deconvolution or resolution of individual component transitions associated with complex DSC curves.²¹⁻²³ Such complex DSC curves can result from multiple two-state transitions, multiple cooperative transitions, sequential transitions, and transitions coupled to association-dissociation processes. By varying the DSC scan rate or a second independent variable (e.g., ligand concentration, pH, or ionic strength), one can obtain a family of heat capacity versus temperature curves. These data can be used to derive kinetic information (e.g., the mean relaxation times as a continuous function of temperature) as well as two-dimensional heat capacity surfaces.^{23a-d} Such surfaces allow one to assess more strictly the validity of various DNA transition models.

It should be clear from the preceding paragraphs that DSC measurements provide an extraordinary wealth of thermodynamic and extrathermodynamic information, much of which cannot be obtained from any other technique. In the paragraphs that follow, we describe how this information can be extracted from the experimental data.

From the area under the experimental C_p^α versus T curve (see Fig. 2), one can calculate the transition enthalpy, ΔH^0 , since $\int C_p dT = \Delta H^0$. Significantly, this calorimetrically determined transition enthalpy is model

¹⁹ B. H. Zimm and J. K. Bragg, *J. Chem. Phys.* **31**, 526 (1959).

²⁰ J. Applequist, *J. Chem. Phys.* **38**, 934 (1963).

²¹ E. Freire and R. L. Biltonen, *Biopolymers* **17**, 463 (1978).

²² E. Freire and R. L. Biltonen, *Biopolymers* **17**, 481 (1978).

²³ E. Freire and R. L. Biltonen, *Biopolymers* **17**, 497 (1978).

^{23a} E. Freire, *Comments Mol. Cell. Biophys.* **6**, 123 (1989).

^{23b} G. Ramsay and E. Freire, *Biochemistry* **29**, 8677 (1990).

^{23c} D. Xie, V. Bhakuni, and E. Freire, *Biochemistry* **30**, 10673 (1991).

^{23d} M. Straume and E. Freire, *Anal. Biochem.*, in press (1992).

independent and therefore does not depend on the nature ("stateness") of the transition. This feature contrasts with model-dependent van't Hoff transition enthalpies which are derived indirectly from the temperature dependence of equilibrium properties.^{15,17,24} Furthermore, from the difference between the initial and final baselines, the DSC measurement also provides a direct measure of the heat capacity change, ΔC_p , accompanying the transition. Consequently, one need not assume that ΔC_p is zero, as frequently is done when analyzing optical data. The experimental C_p^{ex} versus T curve also can be converted to a C_p^{ex}/T versus T curve.²⁴ Because $\Delta S = \int (C_p^{\text{ex}}/T) dT$, the area under such a curve provides a "direct measure" of the entropy change (see Fig. 2b). Thus, from a single DSC transition curve, one can obtain ΔC_p , ΔH^0 , and ΔS^0 . Using these data, the corresponding value of ΔG^0 can be calculated at any temperature (T) using the relationship $\Delta G^0 = \Delta H^0 - T\Delta S^0 = \Delta H_{T_m}[(T_m - T)/T_m] - \Delta C_p(T_m - T) + \Delta C_p T \ln(T_m/T)$. This expression assumes that ΔC_p does not depend on temperature. Although this assumption usually is valid, it is not required to calculate ΔG^0 from the DSC data. It is used here only to simplify the expression.

The calorimetric approach just described for obtaining thermodynamic data on DNA transitions from DSC profiles has two significant advantages relative to van't Hoff methods.^{15,17,24} First, one obtains a model-independent measure of the transition enthalpy and entropy rather than the model-dependent (usually "two-state") values obtained from van't Hoff analyses of equilibrium data. Second, the calorimetric experiment provides a direct measure of ΔC_p so that the temperature dependence of the stability can be assessed.

The DSC data also permit one to evaluate the cooperativity or stateness of a transition.^{15,17,24} This represents a unique advantage of calorimetry. Specifically, comparison of the model-dependent $\Delta H_{v.H.}$ (which can be derived by analyzing the shape of the C_p^{ex} versus T curve) and the model-independent ΔH_{cal} allows one to conclude if the transition proceeds in an all-or-none fashion, thereby providing a test for the applicability of the two-state model to a given transition. If $\Delta H_{v.H.} = \Delta H_{\text{cal}}$, then the transition proceeds in a two-state manner. In such a case, meaningful thermodynamic data can be obtained by monitoring the temperature dependence of an equilibrium property and using the two-state van't Hoff relationship. However, if $\Delta H_{v.H.} < \Delta H_{\text{cal}}$, then the transition involves a significant population of intermediate states, thereby invalidating the use of the simple "all-or-none" analysis. On the other hand, if $\Delta H_{v.H.} > \Delta H_{\text{cal}}$, then intermolecular cooperation (e.g., aggregation) is implicated.

A quantitative comparison of the van't Hoff and calorimetric transition

²⁴ L. A. Marky and K. J. Breslauer, *Biopolymers* **26**, 1601 (1987).

enthalpies provides further insight into the nature of a transition. Specifically, the ratio $\Delta H_{v.H.}/\Delta H_{cal}$ provides a measure of the fraction of the structure that melts as a single thermodynamic entity, in other words, the size of the cooperative unit. This ability to define the size of the cooperative unit represents an important and unique advantage of the calorimetric measurement.

The DSC data also can be used to calculate σ , the cooperativity parameter relevant to the statistical treatments of Zimm and Bragg¹⁹ as well as Applequist.²⁰ Specifically, the maximum value of $C_{p,max}^{ex}$ is proportional to $\sigma^{-1/2}$. The exact relationship²⁵ is given by

$$C_{p,max}^{ex} = (\Delta H)^2 / 4RT^2\sigma^{-1/2} \quad (1)$$

An alternative and somewhat simpler formulation is expressed in the relationship¹⁴

$$\sigma^{-1/2} = m_r \frac{\Delta h_{cal}}{\Delta H_{v.H.}} \quad (2)$$

where m_r is the residue weight of the repeating unit in the DNA polymer and Δh_{cal} is the calorimetric transition enthalpy per gram. Application of either Eq. (1) or Eq. (2) permits one to calculate a value for σ from the calorimetric data. This ability represents yet another unique feature of the information inherent in calorimetric data.

The development of sophisticated analytical procedures has further expanded the information that can be extracted from calorimetric data. In 1978, Freire and Biltonen,²¹⁻²³ showed that the partition function, Q , for a transition can be numerically calculated from the excess heat capacity function by a double integration procedure:

$$\langle \Delta H(T) \rangle = \int_{T_0}^T \langle \Delta C_p \rangle dT \quad (3)$$

$$\ln Q(T) = \int_{T_0}^T \frac{\langle \Delta H \rangle}{RT^2} dT \quad (4)$$

where $\langle \Delta H \rangle$ is the excess enthalpy function. It is well known from statistical thermodynamics that the partition function of a system contains all the information for a complete thermodynamic characterization of a system. This feature has been used to develop deconvolution procedures for evaluating transition mechanisms and for resolving individual components in complex DSC melting profiles. The resulting deconvolution procedure has been used successfully in the analysis of complex DSC profiles for multi-

²⁵ T. Ackermann, in "Biochemical Microcalorimetry" (H. D. Brown, ed.), p. 121 and 235. Academic Press, New York and London, 1969.

domain proteins, nucleic acids, and membrane proteins.^{21-23,26-32a} The original procedure has been improved by the incorporation of multiple passes in the recursive algorithm, each one followed by nonlinear least-squares optimization (see Ref. 31 for a description of the procedure). The incorporation of the nonlinear least-squares routine has allowed the development of programs for the analysis and evaluation of different transition mechanisms such as multiple two-state transitions, multiple cooperative transitions, sequential transitions, and transitions coupled to association-dissociation processes.

Recently, Mayorga and Freire³³ have shown that, by performing DSC measurements at different scan rates, it is possible to estimate mean relaxation times as a continuous function of temperature. The resolution of this method is limited only by the available range of scanning rates and the instrument response time. With the present generation of DSC instruments, relaxation times as fast as 10 sec can be resolved.

Another important focus in the development of new procedures for analysis of DSC data is concerned with transition mechanisms of the form $A \rightleftharpoons B \rightarrow C$, in which the initial conformational equilibrium is followed by an *irreversible* step. Transition mechanisms of this type have been more frequently encountered in protein rather than DNA studies. Nevertheless, it should be noted that under favorable conditions one can extract meaningful thermodynamic information for the equilibrium unfolding step as well as kinetic information for the irreversible step.³⁴ For a critical discussion of methods for evaluating transition mechanisms of this type, see Ref. 34a.

Another important area of DSC data analysis focuses on the development of linked function analysis procedures. These procedures allow one to analyze two-dimensional heat capacity surfaces defined by multiple temperature scans obtained by systematically varying a second independent variable (e.g., ligand concentration, pH, or ionic strength). A global

²⁶ P. L. Privalov, P. L. Mateo, N. Khechinashvili, V. M. Stepanov, and L. Revina, *J. Mol. Biol.* **152**, 445 (1981).

²⁷ P. L. Privalov, *Adv. Protein Chem.* **35**, 1 (1982).

²⁸ P. L. Privalov and L. V. Medved, *J. Mol. Biol.* **159**, 665 (1982).

²⁹ V. Tischenko, V. Zavyalov, G. Medgyesi, S. Potekhim, and P. L. Privalov, *Eur. J. Biochem.* **126**, 517 (1982).

³⁰ T. Tsalkova and P. L. Privalov, *J. Mol. Biol.* **181**, 533 (1985).

³¹ C. Rigell, C. de Saussere, and E. Freire, *Biochemistry* **24**, 5638 (1985).

³² C. Rigell and E. Freire, *Biochemistry* **26**, 4366 (1987).

^{32a} E. Freire and R. L. Biltonen, *Biopolymers* **17**, 1257 (1978).

³³ O. L. Mayorga and E. Freire, *Biophys. Chem.* **87**, 87 (1987).

³⁴ V. Edge, N. M. Allewell, and J. M. Sturtevant, *Biochemistry* **24**, 5899 (1985).

^{34a} E. Freire, W. W. van Osdol, O. L. Mayorga, and J. M. Sanchez-Ruiz, *Annu. Rev. Biophys. Biophys. Chem.* **19**, 159 (1990).

analysis of the data allows for discrimination between various possible transition models. A typical calorimetric scan with data points spaced at intervals of approximately 0.05° contains around 2000 data pairs. Adding a second dimension, for example, 20 different ligand concentrations, increases the total number of data points to 40,000, thereby permitting a far more demanding test of a given transition model.^{23d}

A particularly interesting application in this area is in the study of ligand-DNA interactions. In the simple case where a ligand binds only to the initial duplex state, duplex melting is accompanied by ligand dissociation. Consequently, by comparing the DSC profiles of the ligand-free and ligand-bound duplexes one can determine the enthalpy change associated with ligand "debinding" as well as the influence of the ligand on the melting cooperativity of the duplex state.³⁵ Furthermore, under favorable conditions and in conjunction with the DSC measured transition enthalpy of the free duplex, it is possible to calculate ligand-DNA binding constants from the measured difference in transition temperatures (ΔT_m) of the ligand-free and ligand-bound duplexes.

The theoretical formalism required for such a calculation of binding constants from ΔT_m data has been described by Crothers.³⁶ For the simple case in which the ligand binds only to the initial duplex state the relevant equation is

$$1/T'_m - 1/T_m = R/n\Delta H \ln[1 + Ka_L] \quad (5)$$

where T'_m and T_m are the Kelvin melting temperatures of the DNA duplex in the presence and absence of added ligand, respectively; n is the number of base pairs per ligand at saturation (e.g., $n = 1/r$, where r corresponds to the number of ligands per base pair); ΔH is the transition enthalpy per base pair for the melting of the DNA duplex in the absence of bound drug (a quantity that can be measured directly by DSC); K is the apparent ligand-duplex binding constant at $T = T_m$; a_L is the activity of the free ligand at $T = T_m$, which for strong binding constants ($K > 10^6$) can be approximated by one-half of the total concentration of added ligand (for smaller K values, a_L can be treated as a function of K); and R is the gas constant.

It should be emphasized that a number of implicit and explicit approximations are required for use of Eq. (5) as well as its more general form which describes the ΔT_m relationship for the case in which the ligand binds to both the initial duplex and the final single-stranded states (see Ref. 36). In particular, the ΔT_m equations have been derived assuming a model in which the ligand binds to separate, noninteracting sites on the DNA lattice. One must be cognizant that nonspecific binding as well as ligand aggrega-

³⁵ L. A. Marky, J. G. Snyder, D. P. Remeta, and K. J. Breslauer, *J. Biomol. Struct. Dyn.* **1**, 487 (1983).

³⁶ D. M. Crothers, *Biopolymers* **10**, 2147 (1971).

tion, both of which may depend on temperature and ionic strength, can introduce systematic errors in the ΔT_m analysis. Consequently, the appropriate use of ΔT_m equations requires a healthy respect for and understanding of the approximations employed in its theoretical derivation and its practical application. With an awareness of these considerations, Breslauer and co-workers have demonstrated the utility of the Crothers ΔT_m approach for determining ligand-DNA binding constants from DSC and optical melting data.³⁷⁻⁴¹

Based on the descriptions provided above, it should be clear that DSC studies on DNA can provide an impressive amount of thermodynamic and extrathermodynamic information. To date, only a fraction of this information potential has been tapped in studies of DNA. However, with the increasing availability of high sensitivity DSC instruments coupled with improved methods for DNA synthesis, isolation, and purification, we expect this situation to change rapidly.

Applications

The laboratories of Sturtevant in the United States,⁴²⁻⁴⁷ Ackermann in Germany,⁴⁸⁻⁵³ and Privalov in the Soviet Union⁵⁴⁻⁵⁶ were the first to recognize and to demonstrate the importance of DSC studies on nucleic

- ³⁷ L. A. Marky, J. Curry, and K. J. Breslauer, in "Molecular Basis of Cancer" (R. Rein, ed.), p. 155, Alan R. Liss, New York, 1985.
- ³⁸ J. Snyder, Ph.D. Thesis, Rutgers University, New Brunswick, New Jersey (1985).
- ³⁹ W. Y. Chou, L. A. Marky, D. Zaunczkowski, and K. J. Breslauer, *J. Biomol. Struct. Dyn.* **5**, 345 (1987).
- ⁴⁰ D. P. Remeta, Ph.D. Thesis, Rutgers University, New Brunswick, New Jersey (1989).
- ⁴¹ J. G. Snyder, O. Kennard, N. G. Hartman, B. L. D'Estantoit, D. P. Remeta, and K. J. Breslauer, *Proc. Natl. Acad. Sci. U.S.A.* **86**, 3968 (1989).
- ⁴² M. A. Rawitscher, P. D. Ross, and J. M. Sturtevant, *J. Am. Chem. Soc.* **85**, 1915 (1963).
- ⁴³ I. E. Scheffler and J. M. Sturtevant, *J. Mol. Biol.* **42**, 577 (1969).
- ⁴⁴ H. Krakauer and J. M. Sturtevant, *Biopolymers* **6**, 491 (1968).
- ⁴⁵ J. M. Sturtevant and E. P. Geiduschek, *J. Am. Chem. Soc.* **80**, 2911 (1969).
- ⁴⁶ L. G. Bunville, E. P. Geiduschek, M. H. Rawitscher, and J. M. Sturtevant, *Biopolymers* **3**, 213 (1965).
- ⁴⁷ D. D. F. Shiao and J. M. Sturtevant, *Biopolymers* **12**, 1829 (1973).
- ⁴⁸ T. Ackermann and H. Rueterjans, *Ber. Bunsen-Ges. Phys. Chem.* **68**, 850 (1964).
- ⁴⁹ H. Rueterjans, Ph.D. Thesis, Westfälische Wilhelms Universität, Muenster, Germany (1965).
- ⁵⁰ H. Klump and Th. Ackermann, *Biopolymers* **10**, 513 (1971).
- ⁵¹ H. Klump and W. Burkart, *Biochim. Biophys. Acta* **475**, 601 (1977).
- ⁵² E. Neumann and Th. Ackermann, *J. Phys. Chem.* **73**, 2170 (1969).
- ⁵³ D. Bode, U. Schernau, and T. Ackermann, *Biophys. Chem.* **1**, 214 (1973).
- ⁵⁴ P. L. Privalov, K. A. Kafiani, and D. P. Monaselidze, *Biofizika* **10**, 393 (1965).
- ⁵⁵ P. L. Privalov, O. B. Ptitsyn, and T. M. Birshtein, *Biopolymers* **8**, 559 (1967).
- ⁵⁶ P. L. Privalov, *FEBS Lett.* **40**, 5140 (1974).

acid molecules (see Refs. 10–12, 25, and references cited therein). Their pioneering investigations laid the foundation for much of the subsequent work in this area. However, owing to the poor availability of substantial quantities of highly purified DNA polymers, as well as the near absence of techniques for synthesis of DNA oligomers, these early studies were limited to a small number of synthetic and natural polymers. Nevertheless, it is impressive to note that these original studies have withstood the test of time, despite the substantial technical improvements in DSC instrumentation.

More recently, Breslauer and co-workers have taken advantage of advances in synthetic methodologies to synthesize and to characterize thermodynamically the helix-to-coil transitions for a broad spectrum of specially designed oligomeric and polymeric DNA molecules.^{37,39,41,57–61} (in particular, see Ref. 60) The data from these studies have provided a better understanding of the molecular forces that stabilize DNA structure and have established a thermodynamic library that is being used to predict from the primary sequence the most stable DNA structure under a given set of solution conditions, in other words, the establishment of a phase diagram for DNA. In addition, the resulting thermodynamic data have proved useful in a number of practical applications, such as (1) predicting the stability of probe–gene complexes; (2) selecting optimal conditions for hybridization experiments; (3) deciding on the minimum length of a probe required for hybridization; and (4) predicting the influence of a specific transversion or transition on the stability of an affected DNA region.

Differential scanning calorimetry also has been used to characterize thermodynamically the intramolecular B-to-Z conformational transition in DNA,^{62–64} the thermally induced “unbending” of bent DNA,^{65,65a} the melting of a DNA duplex containing an abasic site,⁶⁶ as well as the melting

- ⁵⁷ L. A. Marky, L. Canuel, R. A. Jones, and K. J. Breslauer, *Biophys. Chem.* **13**, 141 (1981).
- ⁵⁸ D. J. Patel, S. A. Kozlowski, L. A. Marky, C. Broka, J. A. Rice, K. Itakura, and K. J. Breslauer, *Biochemistry* **21**, 428 (1982).
- ⁵⁹ L. A. Marky and K. J. Breslauer, *Biopolymers* **21**, 2185 (1982).
- ⁶⁰ K. J. Breslauer, R. Frank, H. Blöcker, and L. A. Marky, *Proc. Natl. Acad. Sci. U.S.A.* **83**, 3746 (1986).
- ⁶¹ M. M. Senior, R. A. Jones, and K. J. Breslauer, *Proc. Natl. Acad. Sci. U.S.A.* **85**, 6242 (1988).
- ⁶² J. B. Chaires and J. M. Sturtevant, *Proc. Natl. Acad. Sci. U.S.A.* **83**, 5479 (1986).
- ⁶³ H. H. Klump and R. Löffler, *Hoppe-Seyler's Z. Physiol. Chem.* **366**, 345 (1985).
- ⁶⁴ H. H. Klump, *FEBS Lett.* **196**, 175 (1986).
- ⁶⁵ Y. W. Park and K. J. Breslauer, *Proc. Natl. Acad. Sci. U.S.A.* **88**, 1551 (1991).
- ^{65a} K. J. Breslauer, *Curr. Biol.* **1**, 416 (1991).
- ⁶⁶ G. Vesnaver, C.-N. Chang, M. Eisenberg, A. P. Grollman, and K. J. Breslauer, *Proc. Natl. Acad. Sci. U.S.A.* **86**, 3614 (1989).

of single-stranded RNA and DNA sequences.⁶⁷⁻⁷⁰ Such thermodynamic information should prove useful in developing a fundamental understanding of the forces that control DNA structures, as well as in evaluating the energetic role that DNA conformational switches may play in biochemical control mechanisms.

A recent DSC study on oligomeric DNA triplex structures illustrates how calorimetric data can be used to evaluate the influence of sequence, base modification, and solution conditions on triplex stability.⁷¹ Such thermodynamic information is required for the rational design of third-strand oligonucleotides and for defining solution conditions that optimize the effective use of triplex structure formation as a tool for modulating biochemical events. Another recent calorimetric study of tetraplex formation reveals how calorimetric data can be used in conjunction with spectroscopic data to determine the molecularity of a multistrand DNA structure.⁷² This application of DSC data may prove particularly useful in light of the recent excitement over and recognition of the potential importance that higher-order DNA structures may have in biological mechanisms.

As explained above, under favorable conditions, transition temperatures and enthalpies obtained from DSC measurements can be used in conjunction with binding density data to calculate ligand-DNA binding constants. Despite the considerable assumptions inherent in this approach,³⁶ Breslauer and co-workers have shown that the " ΔT_m method" can be used to calculate ligand-DNA binding constants that are in surprisingly good agreement with the values obtained from more traditional methods.³⁷⁻⁴¹ For example, the ΔT_m method yields a binding constant at 25° of $1.5 \times 10^7 M^{-1}$ for complexation of the anthracycline antibiotic daunomycin to the poly[d(AT)]·poly[d(AT)] duplex.⁴⁰ This value is in very good agreement with the corresponding binding constant value of $1.7 \times 10^7 M^{-1}$ determined more conventionally by a Scatchard treatment of fluorescence quenching data.⁴⁰ Breslauer and co-workers have obtained similarly good agreement between K values derived from ΔT_m data and classic binding isotherm data for other DNA-binding ligands such as actinomycin D^{38,41} and two steroid diamines.³⁸ More significantly, the ΔT_m method can be used to determine binding constants for strongly binding

⁶⁷ K. J. Breslauer and J. M. Sturtevant, *Biophys. Chem.* **7**, 205 (1977).

⁶⁸ J. Suurkuusk, J. Alvarez, E. Freire, and R. Biltonen, *Biopolymers* **16**, 2641 (1977).

⁶⁹ V. V. Filimonov and P. L. Privalov, *J. Mol. Biol.* **122**, 465 (1978).

⁷⁰ S. M. Freier, K. O. Hill, T. G. Dewey, L. A. Marky, K. J. Breslauer, and D. H. Turner, *Biochemistry* **20**, 1419 (1981).

⁷¹ G. E. Plum, Y. W. Park, S. Singleton, P. B. Dervan, and K. J. Breslauer, *Proc. Natl. Acad. Sci. U.S.A.* **87**, 9436 (1990).

⁷² R. Jin, K. J. Breslauer, R. A. Jones, and B. L. Gaffney, *Science* **250**, 543 (1990).

ligands for which traditional methods are precluded owing to the low concentration of the free ligand.³⁷

Batch and Stopped-Flow Isothermal Mixing Calorimetry

Method

Until recently, isothermal calorimetric studies on nucleic acid systems primarily have employed batch type, heat conduction instruments. Such instruments basically consist of a bicompartiment cell surrounded by thermoelectric elements embedded within a massive heat sink (see Ref. 73 and articles cited therein). The entire apparatus is kept in a temperature-controlled environment. A typical experiment involves filling each compartment of a bicompartiment cell with aliquots of the reagents of interest. On mixing the two reagents, the liberated or absorbed heat is quantitatively conducted through the surrounding thermopiles to the heat sink. The output of the thermopiles, which measures the rate of heat transfer, is then amplified and recorded. Although quite useful, batch calorimeters suffer from three significant shortcomings: (1) long sample loading and equilibration times between runs ($\sim 1 - 2$ h), thereby limiting the throughput; (2) less than optimum effective sensitivities (~ 60 microjoules, μJ) owing to motion artifacts and mixing problems; and (3) substantial reagent volumes of at least $250 \mu\text{l}$. Titration calorimetry overcomes some, but not all, of these limitations, while also allowing, under favorable circumstances, the determination of binding constants.

A recently developed stopped-flow microcalorimeter⁷⁴ surmounts all of the limitations of conventional batch calorimeters noted above, thereby making it particularly useful in biophysical studies which frequently require high sensitivity and small volumes. A typical stopped-flow microcalorimeter consists of a fluid delivery system, a mixing chamber, flow tubes, a temperature controller, and a massive heat sink. The reagent delivery system is comprised of four thermostatted Hamilton syringes; a computer-controlled stepping motor that delivers $80 \mu\text{l}$ of reagent from each syringe; four flow lines, each connected to a syringe via a three-way valve at its influent end, and welded to one of the two mixing chambers at its terminus; sample and reference mixing chambers embedded in the calorimetric block, each having a total volume of $160 \mu\text{l}$; and two separate flow lines for transporting the reaction products from the mixing chambers

⁷³ C. P. Mudd, R. L. Berger, H. P. Hopkins, W. S. Friauf, and C. Gibson, *J. Biochem. Biophys. Methods* **6**, 179, (1982).

⁷⁴ C. P. Mudd and R. L. Berger, *J. Biochem. Biophys. Methods* **17**, 171 (1988).

to individual collection vials. The reaction is initiated by activating the syringe drive system which delivers 80 μl of each reagent within 0.6 sec into tantalum mixing chambers. Thermopiles surround each mixing chamber and detect the reaction heat that is either liberated or absorbed. As 80 μl of each reactant are used for a 1:1 mixing reaction, a syringe containing 2.5 ml is capable of yielding 30 reactions per filling. In addition, by varying the ratio of the delivered reagents, one can acquire data that correspond to discrete points on a continuous titration curve, as is obtained using isothermal titration calorimetry (see below). The entire instrument is thermostatted so that heat capacity changes (ΔC_p) can be determined by performing ΔH measurements at several temperatures. The technical details that have led these impressive improvements are described in Ref. 74.

Stopped-flow microcalorimeters have been specifically designed and constructed to surmount the limitations normally encountered in conventional batch microcalorimeters. To be specific, the stopped-flow instrument is nearly two orders of magnitude more sensitive than conventional batch microcalorimeters, exhibiting a characteristic sensitivity of 1.595 $\text{J/V}\cdot\text{sec}$. The instrument has a rapid response time (i.e., 10 to 90% in 40 sec), negligible flow artifacts (i.e., less than 2 μJ), and a differential baseline stability of 100 nJ/sec over a 4-hr period. Relative to conventional batch calorimeters, the enhanced sensitivity of the stopped-flow instrument permits significant reductions in the total reaction volume (i.e., 160 versus 1000 μl), limiting reagent concentration (i.e., 20 versus 500 μM), and total run time (i.e., 200 versus 1800 sec). Furthermore, minimization of the reequilibration time between sample sets affords a throughput of 120 to 150 runs per day compared with the 3 to 4 runs typically completed in batch microcalorimetry.

In summary, batch, titration, and stopped-flow calorimeters are all forms of isothermal mixing calorimetry that differ formally only by the means by which one initiates the reaction under study. However, both the titration and stopped-flow modes exhibit significant advantages over the conventional batch instruments.

Information Content

Isothermal mixing calorimetry provides a direct and model-independent measure of the enthalpy change accompanying a chemical reaction. Figure 3 shows a typical "heat burst" curve that is produced on mixing of two reagents. The area under the curve reflects the output voltage of the thermopiles, which is proportional to the total reaction heat, Q_T . In the differential mode, Q_T is obtained by subtracting the measured heat response of the reference chamber from that of the sample chamber and

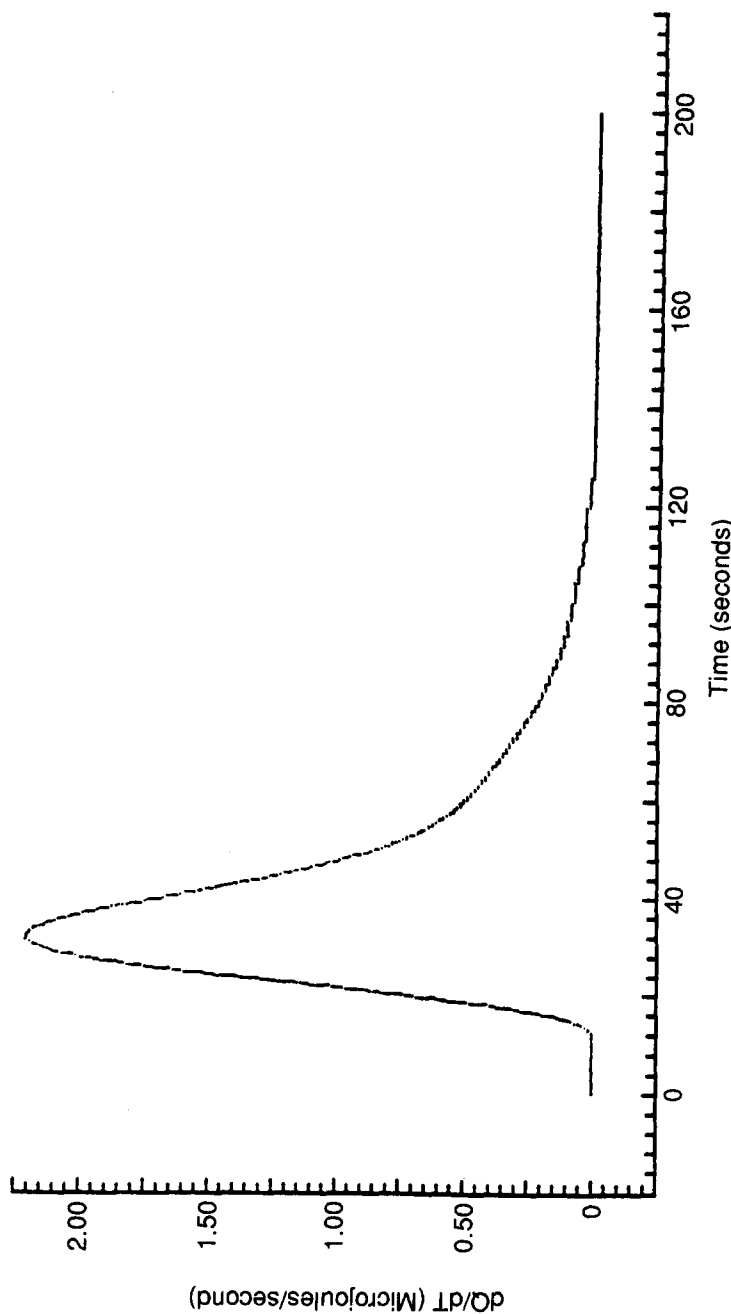


FIG. 3. Stopped-flow microcalorimetric thermogram delineating the exothermic heat evolved for the binding of daunomycin to poly(dAC)]·poly[d(GT)] at a ratio of 1 drug molecule per 20 phosphate residues (D:P = 1:20) at 25°.

integrating the area under the resultant voltage versus time curve according to the relationship

$$Q_T = k \times \text{Area} \quad (6)$$

The proportionality constant, k , required to calculate Q_T is obtained by measuring the area produced by a reaction of known enthalpy. Typical calibration constants of $1.595 \text{ J/V}\cdot\text{sec}$ have been determined for this type of instrument. Knowledge of the reagent concentrations then permits conversion of the observed heat change, Q_T , to an enthalpy change, ΔH . Such directly measured calorimetric enthalpies are more reliable than indirectly derived, model-dependent van't Hoff values. By repeating the isothermal mixing measurement at several temperatures, one also can calculate ΔC_p , the heat capacity change, for the reaction. This much neglected thermodynamic parameter, which for all practical purposes only can be obtained calorimetrically, can provide important insights into the role of solvent in the reaction under study.

The enhanced sensitivity of the stopped-flow microcalorimeter makes it ideally suited not only for isothermal mixing experiments on systems composed of precious material, but also for systems in which one or more of the reagents exhibit concentration-dependent properties. As explained below in the Applications section, drug-DNA binding studies provide good examples of this behavior since many DNA-binding drugs (particularly intercalators) aggregate at the concentrations normally employed in conventional batch calorimetric studies. Under such circumstances, the observed binding heats have to be corrected for the binding-induced disaggregation event. Frequently, this "correction" factor requires the use of van't Hoff enthalpies extracted from temperature-dependent optical studies, thereby compromising the quality of the final "calorimetric" data. The enhanced sensitivity of the recently developed stopped-flow microcalorimeter precludes this problem.

In summary, independent of the mechanical mode by which one initiates a reaction (e.g., titration, batch, stopped-flow) isothermal mixing calorimetry represents the only experimental method that can provide a *direct*, model-independent measure of the enthalpy change, ΔH , and the heat capacity change, ΔC_p , that accompanies an isothermal process.

Applications

Isothermal mixing calorimetry has been used in nucleic acid studies to characterize the influence of metal ion binding; to determine the enthalpy of duplex formation from the mixing of two complementary strands; to measure the energetics of pH-induced changes in nucleic acid structure;

and to determine the enthalpy of small ligand-DNA interactions and protein-DNA interactions.^{35,37,39,40-42,75-93} The case of small ligand-DNA interactions provides a particularly good example for illustrating the advantages of the enhanced sensitivity of the stopped-flow versus the conventional batch calorimeter. Specifically, Breslauer and co-workers have used a conventional batch microcalorimeter to determine the enthalpy change associated with DNA complexation by daunomycin, an intercalating anthracycline antibiotic used in cancer chemotherapy regimens.^{35,85} At the concentrations required for this study, daunomycin aggregates. Consequently, the observed heat changes had to be corrected for binding-induced disaggregation. This correction value was obtained from both temperature-dependent optical studies and temperature-dependent NMR studies.^{35,40,85} Such indirect corrections (which require an assumed model for the aggregation event) compromise the quality of the final enthalpy values. By contrast, the enhanced sensitivity of the stopped-flow microcalorimeter has permitted Breslauer and co-workers to reinvestigate their daunomycin-DNA binding studies at concentrations where the dauno-

- ⁷⁵ G. Rialdi, J. Levy, and R. Biltonen, *Biochemistry* **11**, 2472 (1972).
- ⁷⁶ R. F. Steiner and C. Kitzinger, *Nature (London)* **194**, 1172 (1962).
- ⁷⁷ P. D. Ross and R. L. Scruggs, *Biopolymers* **3**, 491 (1965).
- ⁷⁸ P. D. Ross and R. L. Scruggs, *J. Mol. Biol.* **45**, 567 (1969).
- ⁷⁹ P. D. Ross, R. L. Scruggs, F. B. Howard, and H. T. Miles, *J. Mol. Biol.* **61**, 727 (1971).
- ⁸⁰ R. L. Scruggs and P. D. Ross, *J. Mol. Biol.* **47**, 29 (1970).
- ^{80a} G. Vesnaver and K. J. Breslauer, *Proc. Natl. Acad. Sci. U.S.A.* **88**, 3569 (1991).
- ⁸¹ K. J. Breslauer, G. Charko, D. Hrabar, and C. Oken, *Biophys. Chem.* **8**, 393 (1978).
- ⁸² L. A. Marky, K. S. Blumenfeld, and K. J. Breslauer, *Nucleic Acids Res.* **11**, 2857 (1983).
- ⁸³ L. A. Marky, J. G. Snyder, and K. J. Breslauer, *Nucleic Acids Res.* **11**, 5701 (1983).
- ⁸⁴ L. A. Marky and K. J. Breslauer, *Proc. Natl. Acad. Sci. U.S.A.* **84**, 4359 (1987).
- ⁸⁵ K. J. Breslauer, W. Y. Chou, R. Ferrante, D. Zaunczkowski, J. Curry, D. P. Remeta, J. G. Snyder, and L. A. Marky, *Proc. Natl. Acad. Sci. U.S.A.* **84**, 8922 (1987).
- ⁸⁶ K. J. Breslauer, R. Ferrante, J. Curry, D. Zaunczkowski, R. S. Youngquist, P. B. Dervan, and L. A. Marky, in "Structure and Expression, Volume 2: DNA and Its Drug Complexes" (M. H. Sarma and R. H. Sarma, eds.), p. 273. Adenine Press, Albany, New York, 1988.
- ⁸⁷ C. P. Mudd, R. L. Berger, D. P. Remeta, and K. J. Breslauer, *Biophys. J.* **53**, 480a (1988).
- ^{87a} D. P. Remeta, C. P. Mudd, R. L. Berger, and K. J. Breslauer, *Biochemistry* **30**, 9799 (1991).
- ⁸⁸ Y. Takeda, P. D. Ross, and C. P. Mudd, *Biophys. J.* **57**, 225a (1990).
- ⁸⁹ M. Lee, R. G. Shea, J. A. Hartley, K. Kissinger, R. T. Pon, G. Vesnaver, K. J. Breslauer, J. C. Dabrowiak, and J. W. Lown, *J. Am. Chem. Soc.* **111**, 345 (1989).
- ⁹⁰ R. Jin and K. J. Breslauer, *Biophys. J.* **55**, 374a (1989).
- ⁹¹ D. P. Remeta and K. J. Breslauer, *Conv. Biomol. Stereodyn.* **6**, 275a (1989).
- ⁹² M. Lee, R. G. Shea, J. A. Hartley, K. Kissinger, G. Vesnaver, K. J. Breslauer, R. T. Pon, J. C. Dabrowiak, and J. W. Lown, *J. Mol. Recognit.* **2**, 6 (1989).
- ⁹³ F. Quadrifoglio and V. Crescenzi, *Biophys. Chem.* **2**, 64 (1974).

mycin exists in the monomeric state, thereby precluding the need to correct the observed heat effects for drug dissociation.^{40,85,87,87a}

The enhanced sensitivity of the stopped-flow instrument also has permitted Breslauer and colleagues to evaluate if the daunomycin binding enthalpies exhibit a dependence on the ligand-to-DNA ratio (the so-called *r* value).^{87a} In cases of cooperative ligand binding, this capability provides an opportunity to evaluate the thermodynamic basis for this intriguing binding phenomenon. In fact, a recent stopped-flow microcalorimetric study on daunomycin binding to a variety of synthetic and natural DNA duplexes reveals the binding enthalpies to vary with the *r* values in a manner that depends on both base composition and base sequence.^{40,87,87a} The measurements required to make such an assessment would have been difficult, if not impossible, to perform using conventional batch calorimeters.

A very recently published study^{80a} illustrates the power of using both differential scanning and batch calorimetric techniques to characterize thermodynamically the forces that control DNA structures. Specifically, Vesnaver and Breslauer^{80a} have used DSC to characterize the thermally induced *disruption* of a DNA duplex and its component single strands, while also using isothermal mixing calorimetry to characterize the *formation* of the same duplex from its component single strands. The data obtained from these measurements allowed construction of a thermodynamic cycle which revealed that single-stranded order can contribute significantly to the thermodynamics of duplex formation. This feature must be recognized and accounted for when designing single-strand probes for selective DNA hybridization experiments and when interpreting thermodynamic data associated with the formation of higher-order DNA structures (e.g., duplexes, triplexes, tetraplexes, etc.) from inter- and/or intramolecular associations of single strands.

Isothermal Titration Calorimetry

Method

In a differential isothermal titration calorimeter (ITC), two titration cells reside in the calorimeter assembly, one reference and one sample. Detection of heat effects in titration microcalorimeters is generally accomplished by use of semiconductor thermopiles interposed between the reaction cell(s) and a constant temperature heat sink. A typical calorimetric titration will involve having the reference cell filled with buffer only and the sample cell with buffer plus the reactant to which ligand will be titrated. Identical injections of ligand are introduced into both mechanically stirred

titration cells by a dual-injection mechanism. Heat effects measured in the reference cell arise from injection and dilution of the ligand. Heat effects measured in the sample cell arise from injection and dilution of ligand as well as from the reaction of interest. The difference between the heat effects in both cells is then equal to the heat of reaction. This measured heat of reaction is proportional to the product of the amount of ligand bound and the enthalpy change for the binding process.

Heat flow between the titration cell(s) and the heat sink occurs only through the thermopile thermal detectors, the voltage output of which is directly proportional to the temperature difference across the faces of the thermopiles. This temperature difference, in turn, is proportional to the thermal power being exchanged between the titration cell(s) and heat sink [rate of heat transfer (cal sec^{-1})].⁹⁴

The instrumental response time can be made approximately an order of magnitude faster by employing power compensation to drive the system actively toward the steady-state baseline condition. New ultrahigh sensitivity ITCs using this principle are characterized by instrument response times of the order of 10–15 sec compared to 100–300 sec for older instrumentation.⁹⁴ Because the total heat associated with reaction is the time integral of the observed thermal power released or absorbed (as shown in Fig. 4), reducing the time response provides more sensitive detection of total heat effects per injection. The thermal power signal-to-noise ratio is increased with power compensation because of the greater thermal power amplitude needed to generate the same total heat (area under the curve) in a shorter period of time.

In a power compensation ITC, the directly recorded quantity is the amount of thermal power that must be applied to actively compensate the heat of reaction induced by injection. This is accomplished by continuously regulating the amount of heat applied to the titration cell(s) so as to drive the measured thermal power amplitude toward the steady-state, baseline value. In practice, this is accomplished via an interfaced computer that monitors the output of a nanovoltmeter connected to record the voltage developed by the thermopiles. Real-time adjustments to the current applied to resistive cell feedback elements associated with the reaction cell(s) are then dynamically controlled by software to provide active power compensation of the detected change in thermopile output. The applied thermal power as a function of time required to return the ITC to its steady-state condition following injection then becomes the direct experimentally determined quantity that is proportional to the heat of reaction.

⁹⁴ E. Freire, O. L. Mayorga, and M. Straume, *Anal. Chem.* **52**, 950A (1990).

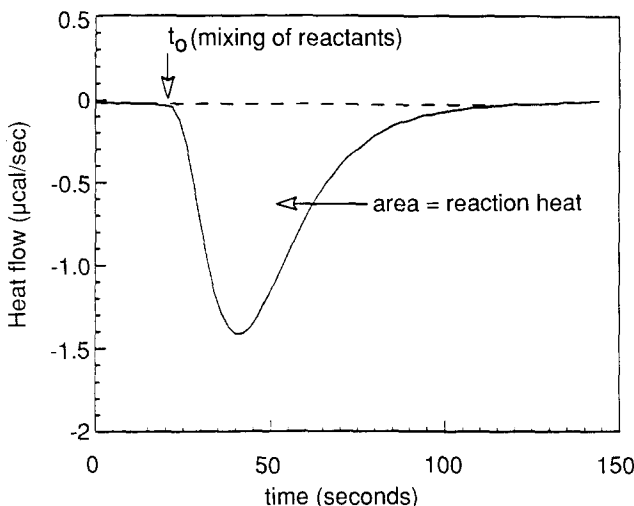


FIG. 4. Typical isothermal titration calorimetric trace. At time t_0 , one of the reactants is injected into the calorimeter cell already containing the other reactant. The heat effects associated with the reaction are measured continuously as a function of time. The area under the curve is equal to the heat absorbed (positive) or released (negative) during the reaction. When normalized by the amount reacted, it yields directly the enthalpy for the reaction.

Information Content

The association of biological macromolecules to one another as well as their association to small ligand molecules play a central role in the structural assembly and functional regulation of many biological systems. Quantitative characterization of the thermodynamics of such molecular interactions is of fundamental importance for developing a thorough understanding of how biological function is regulated by ligand binding or molecular associations. A comprehensive understanding of the energetics associated with molecular interactions requires information about the thermodynamic parameters that define intrinsic binding events as well as any associated cooperative effects brought on by binding. Calorimetric titration experiments designed to characterize quantitatively the energetics of ligand-linked macromolecular cooperativity will provide considerable insight into the molecular basis of information transfer with macromolecules via cooperative effects.

Isothermal titration calorimetry measures the energetics of biochemical reactions or molecular interactions at constant temperature. The observed quantity is the amount of heat released or absorbed by the process. A broad range of molecular processes, such as ligand binding phenomena (e.g.,

protein–nucleic acid interactions, drug–nucleic acid interactions, hormone–receptor interactions, enzyme–substrate interactions, binding of substrates or substrate analogs, and cofactor binding) as well as interactions among components of multimolecular complexes (e.g., multisubunit enzyme complexes, multimolecular aggregates, and protein–membrane interactions), may be characterized by application of ITC.

Since the mid-1980s, ITC has experienced tremendous advances in sensitivity owing to the incorporation of microelectronics and new instrument designs. In the past, the use of ITC was somewhat limited owing to a lack of sufficient sensitivity for characterization of high affinity binding reactions. Such experiments require dilute reactant concentrations in order to determine equilibrium constants accurately. These limitations no longer exist given the recent development of instruments capable of measuring heat effects from reactions involving nanomoles or less of reactants.^{94–101}

The new generation of titration calorimeters makes possible direct thermodynamic characterization of association processes exhibiting the very high affinity binding constants frequently encountered in biological systems, particularly those involved in regulation of function. Direct calorimetric titration experiments may be used to define fully the thermodynamics of both (1) intrinsic ligand binding as well as (2) any ligand-induced cooperative effects. The ability to measure small heats of reaction (of the order of 10^{-7} – 10^{-6} cal/ml of solution) allows direct calorimetric examination of binding processes with K_a values as high as 10^8 – $10^9 M^{-1}$ (requiring dilute reactant concentrations of $\sim 10^{-6} M$ or less). Additionally, the recent development of an approach, total association at partial saturation (TAPS), for experimentally uncoupling intrinsic ligand binding energetics from those associated with ligand-induced macromolecular cooperative effects provides a direct calorimetric means for probing the molecular origins of information transduction within macromolecular structures.

Figure 4 presents a typical calorimetric titration response in which the thermal power versus time is measured. At time t_0 (the time of injection), titrant is introduced to the sample, producing an exothermic system response (i.e., a release of heat as indicated by the negative deflection of the thermal power). The area encompassed by the curve is the reaction heat

⁹⁵ R. B. Spokane and S. J. Gill, *Rev. Sci. Instrum.* **52**, 1728 (1981).

⁹⁶ J. Donner, M. H. Caruthers, and S. J. Gill, *J. Biol. Chem.* **257**, 14826 (1982).

⁹⁷ I. R. McKinnon, L. Fall, A. Parody, and S. J. Gill, *Anal. Biochem.* **139**, 134 (1984).

⁹⁸ G. Ramsay, R. Prabhu, and E. Freire, *Biochemistry* **25**, 2265 (1986).

⁹⁹ M. Myers, O. L. Mayorga, J. Emtage, and E. Freire, *Biochemistry* **26**, 4309 (1987).

¹⁰⁰ A. Schon and E. Freire, *Biochemistry* **28**, 5019 (1989).

¹⁰¹ T. Wiseman, S. Williston, J. F. Brandts, and L.-N. Lin, *Anal. Biochem.* **179**, 131 (1989).

which, when normalized for the amount of material undergoing reaction, produces directly the enthalpy of reaction. In addition to defining the total heat associated with an injection event (as the area under the thermal power versus time curve), the time decay of the signal, after correction for instrument response, is related to the kinetics of the process.³³ The existence of multiple kinetic phenomena (e.g., slow structural rearrangement following binding) will result in a complex time dependence of the thermal power signal.

Quantitation of Binding Equilibria

Quantitative characterization of the energetics of molecular associations is commonly performed by analysis of binding isotherms. In this approach, ligand-binding macromolecules are sequentially titrated to completion under experimental conditions that permit extraction of all of the thermodynamic parameters that define the binding process. The characterization of the binding of a ligand molecule to a macromolecule requires the determination of the association constant, K_a , or the Gibbs free energy of association, $\Delta G^0 = -RT \ln K_a$, as well as the enthalpic and entropic contributions to the overall binding free energy ($\Delta G^0 = \Delta H^0 - T\Delta S^0$). Further determination of the temperature dependence of the enthalpy change permits estimation of the changes in heat capacity [$\Delta H = \Delta H^0 + \Delta C_p(T - T^0)$]. For those cases in which more than one binding site exists in the macromolecule, it is necessary to assess whether the sites are independent (or noninteracting) or whether the occupancy of one or more of them affects the ligand affinity of the remaining unligated sites. Interacting binding sites give rise to cooperative ligand binding behavior, a critically important general mechanism employed by a broad diversity of biological macromolecules to regulate functional responses. In these cases, it is important to determine the energetics of the cooperative interactions as defined by interaction free energy, enthalpy, and entropy changes. The major goal of the calorimetric approach to the analysis of ligand-binding phenomena is the determination of the intrinsic binding energetics as well as the cooperative energetics. Different strategies have been devised to achieve these goals, as described below.

The most common approach is the generation of a ligand-binding isotherm. In the calorimetric situation, the isotherm is defined in terms of the amount of heat that is released (exothermic) or absorbed (endothermic) as a function of the total concentration of ligand in the solution. Thermodynamic parameters (ΔG^0 , ΔH^0 , ΔS^0) are estimated by linear or nonlinear least-squares analysis of the binding isotherm, much the same as for other techniques. In the case of cooperative binding, the interaction parameters

have to be included in the fitting as well. However, when analysis of ligand-binding isotherms is performed to extract cooperative interaction energy terms simultaneously with those characteristic of the intrinsic binding process, the mathematical correlation among model fitting parameters may become a formidable problem.¹⁰² Experimental uncoupling of cooperative ligand binding energetics from those associated with intrinsic ligand binding, as is the case with TAPS (see below), permits a more robust parameter estimation free of the parameter correlation effects encountered when analyzing complete binding isotherms for intrinsic as well as cooperative effects.

Total association at partial saturation (TAPS), an approach unique to calorimetric titrations, alleviates the problems of parameter correlation mentioned above and directly quantifies ligand-induced cooperative effects independent of the influences of intrinsic binding.¹⁰³ Experiments in this case are performed under conditions of TAPS by titrating macromolecular ligand binding sites that are present at concentrations greater than K_d for the reaction. This ensures that all of the ligand introduced into the reaction cell by titration will bind to the available binding sites. At the point at which all acceptor sites are saturated, no further reaction occurs. These conditions make the dependence of the observed apparent binding enthalpy on extent of saturation with ligand a function of only the cooperative energetics of ligand binding. Because concentrations of macromolecular binding sites must be at least about 10^3 greater than K_d for the reaction, this technique provides direct experimental access to the cooperative binding energetics of systems with K_a exceeding approximately $10^9 - 10^{10} M^{-1}$ by uncoupling the energetics of cooperative interactions from those associated with intrinsic binding. For positive cooperativity, TAPS normally produces reliable parameter estimates, even if the initial concentration of binding sites is only 10^2 times larger than the K_d . For negative cooperativity, the situation is different and care must be taken because the drop in affinity may abolish the conditions for TAPS.

Binding Equilibrium Evaluated from Ligand-Binding Isotherms

A variety of mathematical procedures have been devised to estimate association constants, numbers of binding sites, and cooperative interactions from ligand-binding isotherms. Linearized transforms of ligand-binding data, such as the Scatchard plot (in which the ratio of bound to free ligand is plotted versus bound ligand), have been extremely widely used. Such transformations, however, produce biases in the analysis because the

¹⁰² M. Straume and M. L. Johnson, *Biophys. J.* **56**, 15 (1989).

¹⁰³ G. Bains and E. Freire, *Anal. Biochem.* **192**, 203 (1991).

distinction between dependent and independent variables is obscured. Direct nonlinear least-squares analysis of the dependent versus independent variable(s) provides a statistically more accurate estimation of model parameter values free of the implicit biases that arise in analysis of (nonlinear) transformed data.^{102,104–106}

On binding of ligand to a macromolecule, heat is released or absorbed as a result of the binding event (owing to the enthalpy of ligand binding). The heat effects measured for each addition of ligand represent the experimentally observed response in ITC experiments and are described by

$$q = V\Delta H\Delta[L_B] \quad (7)$$

where q is the heat associated with the change in bound ligand concentration, $\Delta[L_B]$ is the change in bound ligand concentration, ΔH is the enthalpy of binding in (moles ligand)⁻¹, and V is the reaction volume.

Because the observed heat, q , is proportional to the increase in bound ligand concentration, the magnitude of q decreases as the system is titrated to completion. This is demonstrated in Fig. 5, where an example of a calorimetric titration of RNase A with 2'-CMP at 25° is presented. The heat effects associated with successive injections of 2'-CMP are seen to decrease in amplitude as the RNase A present in the sample cell is titrated to completion. The total cumulative heat released or absorbed is proportional to the total concentration of bound ligand:

$$Q = V\Delta H \sum \Delta[L_B] = V\Delta H[L_B] \quad (8)$$

where Q is the cumulative heat and $[L_B]$ is the concentration of bound ligand.

Analysis of binding isotherms in terms of the multiple sets of independent binding sites model^{107,108} offers a general, flexible framework to extract information about a great variety of ligand-binding situations. Single or multiple binding sites, multiple sets of binding sites, as well as positive and negative cooperative effects may, in principle, all be accommodated by this model. The model assumes that the ligand-binding macromolecule possesses an arbitrary number of sets of noninteracting binding sites, and that all sites in the same set possess the same affinity for ligand. The concentration of ligand bound to each set of binding sites, as given by this

¹⁰⁴ M. L. Johnson, *Biophys. J.* **44**, 101 (1983).

¹⁰⁵ M. L. Johnson, *Anal. Biochem.* **148**, 471 (1985).

¹⁰⁶ M. Straume and M. L. Johnson, *Biochemistry* **27**, 1302 (1988).

¹⁰⁷ K. E. van Holde, in "Physical Biochemistry," 2nd Ed., Chap. 3. Prentice-Hall, Englewood Cliffs, New Jersey, 1985.

¹⁰⁸ C. R. Cantor and P. R. Schimmel, in "Biophysical Chemistry, Part III: The Behavior of Biological Macromolecules," Chap. 15. Freeman, New York, 1980.

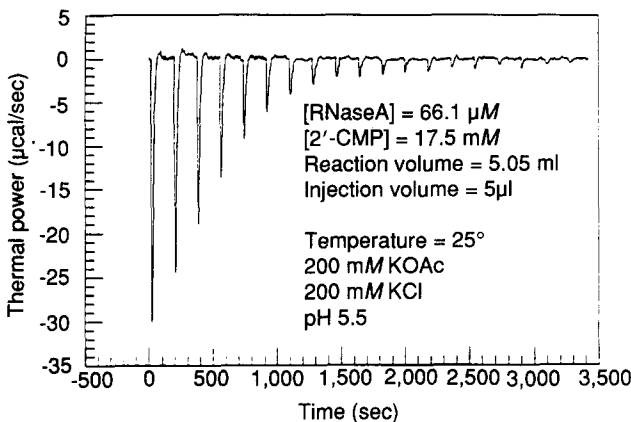


FIG. 5. Calorimetric titration of RNase A with 2'-CMP, showing the calorimetric response as successive injections of ligand are added to the reaction cell. As the binding sites become saturated with ligand, the magnitude of the heat effects decreases, becoming negligible as full saturation is approached.

model, is

$$[L_{B,i}] = [M] \frac{n_i K_i [L]}{1 + K_i [L]} \quad (9)$$

where $[L_{B,i}]$ is the concentration of ligand bound to binding sites of set i , $[M]$ is the total concentration of macromolecule available for binding ligand, K_i is the intrinsic site association constant for binding sites of set i , n_i is the number of binding sites of set i on each macromolecule M , and $[L]$ is the concentration of free ligand. Because the heat associated with the binding event is proportional to the concentration of bound ligand, $[L_B]$, the cumulative amount of heat released or absorbed is then given by the sum of the heats corresponding to each set:

$$Q = V \sum_i \Delta H_i [L_{B,i}] = V[M] \sum_i \frac{n_i \Delta H_i K_i [L]}{1 + K_i [L]} \quad (10)$$

where ΔH_i is the enthalpy of binding in $(\text{moles ligand})^{-1}$ to binding sites of set i .

Equations (7) through (10) must be considered in terms of total ligand concentration by use of the expression $[L_T] = [L_B] + [L]$ (where $[L_T]$, $[L_B]$, and $[L]$ correspond to the concentrations of total, bound, and free ligand, respectively). The variable model parameters n_i , K_i , and ΔH_i are then estimated by nonlinear least-squares analysis of the calorimetric titration data. Either the cumulative heat, Q , or the individual heat, q , may be

considered in the parameter estimation process. However, analysis of the individual heats, q_i , is preferable because the uncertainties associated with each injection, σ_{q_i} , are not propagated as is the case with cumulative heat data. Figure 6 presents an analysis of the calorimetric titration experiment presented in Fig. 5 for the binding of 2'-CMP to RNase A by application of the above model. In this case, the model parameters that must be estimated are the binding enthalpy (ΔH) and the binding affinity (as determined by the ligand association constant, K_a , or the free energy of ligand binding, $\Delta G^0 = -RT \ln K_a$).

Cooperative Energetics as Determined by Total Association at Partial Saturation

Calorimetric titrations conducted under conditions of total association at partial saturation allow direct calorimetric visualization of cooperative

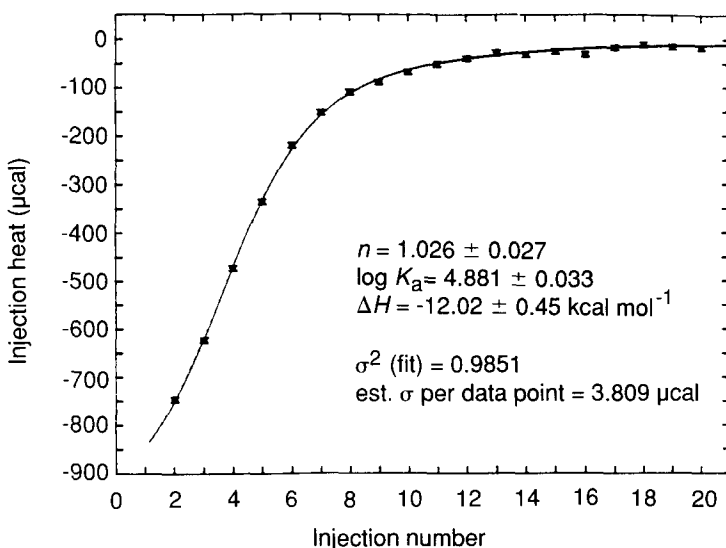


FIG. 6. Results of analysis of the calorimetric titration of RNase A with 2'-CMP shown in Fig. 5 presented as individual injection heats as a function of injection number. The curve represents the nonlinear least-squares best fit of the data. The results indicate the existence of one 2'-CMP binding site (1.026 ± 0.027) with a binding association constant K_a of $7.60 (\pm 0.58) \times 10^4 M^{-1}$ at 25° and a reaction enthalpy of $-12.02 \pm 0.45 \text{ kcal mol}^{-1}$. The derived variance of fit is 0.9851, indicating a satisfactory fit (i.e., the variance of fit is less than 1). The estimated standard deviation per data point was $3.809 \mu\text{cal}$ as determined from electrical calibration measurements performed in conjunction with the calorimetric titration. Because the reaction volume is 5.05 ml , this translates to a specific instrumental sensitivity of $0.754 \mu\text{cal ml}^{-1}$.

interactions without interferences from the binding event per se.¹⁰³ Because relatively high concentrations of the ligand-binding macromolecule are needed to satisfy this condition ($\sim K_d \times 10^3$ or more), cooperative interaction energies may be determined directly even for those cases in which the ligand affinity is extremely high and cannot be determined directly (i.e., for those cases with K_a values greater than $\sim 10^9 M^{-1}$).

The example of a macromolecule possessing two ligand binding sites will suffice to demonstrate the principle and application of TAPS. A model for ligand binding to such a macromolecule must account for the intrinsic binding properties of the binding sites ($-RT \ln K_a = \Delta G^0 = \Delta H^0 - T\Delta S^0$) as well as allow for ligand-linked cooperative interactions ($\Delta g = \Delta h - T\Delta s$) induced by binding of the first ligand. As shown in Fig. 7, the relative free energies of all accessible states of this ligand-binding system are given by (1) a singly degenerate unliganded reference state with $\Delta G_0 = 0$, (2) a doubly degenerate singly liganded state with $\Delta G_1 = \Delta G^0$, and (3) a singly degenerate fully liganded state with $\Delta G_2 = 2\Delta G^0 + \Delta g$. The corresponding relative enthalpies of each of these system states are given by (1) $\Delta H_0 = 0$ for the singly degenerate unliganded reference state, (2) $\Delta H_1 =$

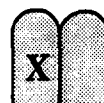
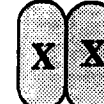
STATE	LIGANCY	FREE ENERGY	ω	S.W.
0		Ref.	1	1
1		ΔG	2	$2 K [X]$
2		$2 \Delta G + \Delta g$	1	$k K^2 [X]^2$

FIG. 7. Complete representation of the thermodynamic parameters necessary to define fully both the intrinsic and cooperative ligand-binding energetics of a ligand-binding macromolecule possessing two, interacting binding sites. The free energy, degeneracy (ω), and statistical weight for each accessible state of the system are presented. The objective of calorimetric titrations under conditions of TAPS is to quantify directly, experimentally the cooperative energetics associated with ligand binding (i.e., Δg , Δh , and Δs ; see text for additional details). Reproduced from Fig. 1 of Ref. 103.

ΔH^0 for the doubly degenerate singly liganded state, and (3) $\Delta H_2 = 2\Delta H^0 + \Delta h$ for the singly degenerate fully liganded state. An interaction free energy (Δg) of zero produces two independent sites, the affinities of which are unaffected by the state of ligand occupancy of the other site. However, a negative Δg produces positive cooperativity by increasing the affinity for the second ligand, whereas a positive Δg causes reduced affinity for the second ligand, resulting in negatively cooperative binding.

Both the interaction free energy (Δg) and the interaction enthalpy (Δh) can be determined from the dependence of the observed apparent binding enthalpy ($\langle \Delta H \rangle$) on the degree of binding saturation under conditions of total association at partial saturation (TAPS). As demonstrated in Fig. 8, the observed enthalpy of binding approaches the intrinsic binding enthalpy (ΔH^0 assumed to be $-30 \text{ kcal mol}^{-1}$) at low degrees of saturation, whereas at full saturation the observed enthalpy of binding is the average over both sites [$(2\Delta H^0 + \Delta h)/2$, with a Δh of $-10 \text{ kcal mol}^{-1}$]. The dependence of $\langle \Delta H \rangle$ on the degree of saturation is determined solely by the magnitude

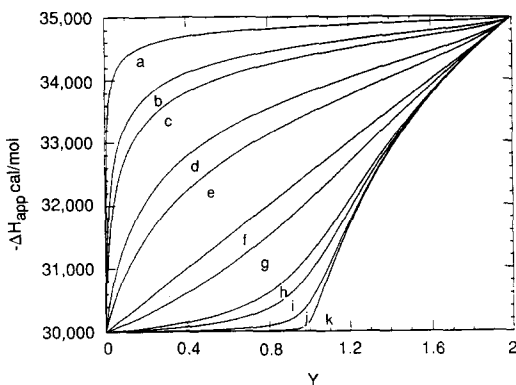


FIG. 8. Dependence of the apparent binding enthalpy for a ligand-binding macromolecule possessing two, interacting binding sites presented as a function of the degree of ligand saturation for a variety of cooperative interaction free energies. The intrinsic enthalpy of binding (ΔH) is assumed for this simulation to be $-30 \text{ kcal mol}^{-1}$, whereas a cooperative interaction enthalpy (Δh) of $-10 \text{ kcal mol}^{-1}$ is assumed. The statistical thermodynamic partition function for this system is given by $Z = 1 + 2K[X] + kK^2[X]^2$ where $K = \exp(-\Delta G/RT)$ and $k = \exp(-\Delta g/RT)$. The ligand saturation function is then $Y = (1/Z)(2K[X] + 2kK^2[X]^2)$, and the apparent binding enthalpy ($\langle \Delta H \rangle$) is given by $\langle \Delta H \rangle = (1/Z)(2K[X]\Delta H + kK^2[X]^2(2\Delta H + \Delta h))$. A range of k values from 1000 (positive cooperativity, negative Δg) to 0.001 (negative cooperativity, positive Δg) are considered with $k = 1$ representing the case of independent sites (i.e., no cooperativity associated with ligand binding). The values of k are as follows: (a) 1000, (b) 100, (c) 50, (d) 10, (e) 5, (f) 1, (g) 0.5, (h) 0.1, (i) 0.05, (j) 0.01, and (k) 0.001. Reproduced from Fig. 3 of Ref. 103.

and sign of the interaction free energy (Δg), whereas the magnitude of $\langle \Delta H \rangle$ is related to both ΔH^0 and Δh . Thus, at any given degree of saturation, the distribution of accessible system states will be determined by the energetics of the cooperative interactions. This distribution may be obtained experimentally by nonlinear least-squares analysis of the observed dependence of $\langle \Delta H \rangle$ on degree of macromolecular ligand saturation. Knowledge of the parameter values for ΔH , Δh , and Δs then fully defines the experimental observations under conditions of TAPS in terms of the ligand-linked cooperative binding energetics characteristic of the ligand-binding macromolecule.

Cooperative effects associated with ligand binding are thought to arise from ligand-induced protein conformational changes. Isothermal titration calorimetry, by employing TAPS, allows direct measurement of the energetics of the cooperative interactions and putative conformational changes independent of the intrinsic binding energetics. Complementary analysis of complete ligand-binding isotherms provides quantitation of the thermodynamics of the intrinsic binding process(es), as well. Comprehensive studies of this type will permit direct characterization of the nature and magnitude of the forces associated with many different biomolecular interactions. Calorimetric titrations of the sort described may prove to be particularly useful, for example, in screening of mutant forms of ligand-binding macromolecules created by genetic means as well as in characterization of the effects of amino acid substitutions on the thermodynamics of protein stability and interaction with ligands or other proteins. Ultimately, this type of comprehensive thermodynamic information will contribute to identification of the sequence of molecular events involved in transduction and regulation of biological information in a wide range of systems.

Applications

Many nucleic acid-binding proteins and macromolecular assemblies exhibit very high binding affinities as well as cooperative effects associated with the binding process. These may take the form of cooperative macromolecular structural changes induced by binding of small regulatory ligands which in turn modify the macromolecular binding affinity for a nucleic acid regulatory site, as in the case of regulation by *lac* repressor, for example.¹⁰⁹ Other systems exhibit long-range cooperative effects as a result of nearest-neighbor interactions among adjacent protein molecules bound to single-stranded nucleic acids (e.g., bacteriophage T4 gp32¹¹⁰). The *Esch-*

¹⁰⁹ A. Revzin, in "The Biology of Nonspecific DNA-Protein Interactions" (A. Revzin, ed.), Chap. 4. CRC Press, Boca Raton, Florida, 1990.

¹¹⁰ R. L. Karpel, in "The Biology of Nonspecific DNA-Protein Interactions" (A. Revzin, ed.), Chap. 5. CRC Press, Boca Raton, Florida, 1990.

erichia coli single-stranded binding protein (*EcoSSB*) has been quite extensively characterized^{111–113} and has been shown, by spectroscopic methods, to exhibit multiple types of cooperative single-stranded nucleic acid binding behavior that is strongly coupled to environmental ionic strength.

A higher order level of molecular association phenomena must be considered in cases of regulation in multimolecular aggregates. The affinity of cAMP receptor protein (CRP) for nucleic acids is influenced by binding of cAMP (a regulatory ligand that modifies the affinity of CRP for nucleic acids).¹¹⁴ CRP, in turn, is implicated as potentially interacting in a regulatory manner with other nucleic acid-binding enzymes, thus modifying their activity, possibly through communication via protein–protein contacts. A great many examples of protein–nucleic acid interacting systems exist for which knowledge of the thermodynamic mechanisms underlying ligand binding or macromolecular association will contribute to elucidating the molecular basis for functional regulation of genetic expression.^{115–117} Thermodynamic characterization of both the intrinsic binding or association process(es) and the cooperative energetics associated with any cooperative structural changes will shed light on the molecular origins of regulatory communication pathways.

Multifrequency Calorimetry

Method

The calorimetric techniques discussed above are all designed to measure the equilibrium thermodynamics associated with structural transformations or macromolecular interactions with ligands or other macromolecules. Recently, a new type of calorimetry aimed at measuring the dynamics or kinetics of the energetics of macromolecular transitions has been introduced.^{118–120} This technique, multifrequency calorimetry, per-

¹¹¹ T. M. Lohman and W. Bujalowski, in "The Biology of Nonspecific DNA–Protein Interactions" (A. Revzin, ed.), Chap. 6. CRC Press, Boca Raton, Florida, 1990.

¹¹² J. Greipel, C. Urbanke, and G. Maass, in "Protein–Nucleic Acid Interactions" (W. Saenger and U. Heinemann, eds.), Chap. 4. CRC Press, Boca Raton, Florida, 1989.

¹¹³ J. W. Chase and K. R. Williams, *Annu. Rev. Biochem.* **55**, 103 (1986).

¹¹⁴ S. Garge and S. Adhya, *Cell (Cambridge, Mass.)* **41**, 745 (1985).

¹¹⁵ P. H. von Hippel and O. G. Berg, in "Protein–Nucleic Acid Interactions" (W. Saenger and U. Heinemann, eds.), Chap. 1. CRC Press, Boca Raton, Florida, 1989.

¹¹⁶ C. R. Vinson, P. B. Sigler, and S. L. McKnight, *Science* **246**, 911 (1989).

¹¹⁷ R. Schleif, *Science* **241**, 1182 (1988).

¹¹⁸ O. L. Mayorga, W. van Osdol, J. L. Lacomba, and E. Freire, *Proc. Natl. Acad. Sci. U.S.A.* **85**, 9514 (1988).

¹¹⁹ E. Freire, *Comments Mol. Cell. Biophys.* **6**, 123 (1990).

¹²⁰ O. L. Mayorga, W. van Osdol, and E. Freire, *Biophys. J.* **59**, 48 (1991).

mits a determination of the time regime in which the energy transformations take place, allowing the assignment of time constants to the enthalpic events associated with a reaction.

The idea behind multifrequency calorimetry is simple even though the mathematical formulation is somewhat cumbersome and will not be discussed here (the reader is referred to Ref. 34a for a complete review). Basically, a multifrequency calorimeter is composed of a very thin, disk-shaped, sample compartment (0.1–1 mm thick) in which the macromolecular solution is placed. On one face of the disk-shaped cell (the excitation side) a battery of miniature Peltier elements generate a periodic temperature oscillation. This oscillation can be a simple sine wave, a superposition of harmonics, or a more complex waveform. The amplitude of the temperature oscillation is usually of the order of 0.05°. On the opposite side of the sample cell (the measurement side) the response temperature oscillation after the wave has traveled through the solution is measured. The response wave is attenuated in amplitude and phase shifted with regard to the excitation wave. The magnitude of these changes are a function of the excitation frequency and depend on instrument parameters (e.g., cell thickness), intrinsic solution parameters (e.g., heat capacity of the solution), and the thermodynamic and kinetic parameters associated with the transition under consideration. Instrumental designs and data analysis procedures are directed to extract the parameters associated with the transition.

Information Content

Multifrequency calorimetry is particularly important for the analysis of complex transitions involving intermediate states. In protein folding studies, for example, conventional calorimetry has become the technique of choice for thermodynamic analysis owing to its ability to provide extremely precise and model-independent estimates of the overall energetics of the process. Contrary to the thermodynamic analysis, the kinetic analysis of protein folding has relied primarily on a variety of observables that report time-dependent changes of some system property as the system evolves from the folded to the unfolded state or vice versa. Because physical observables are often sensitive only to local properties of the molecule, it is a common occurrence for different physical observables to report distinct numbers of relaxation processes and amplitudes. In general, those relaxation processes cannot be correlated directly with the dynamics of the enthalpic events associated with the folding/unfolding transition. The goal of multifrequency calorimetry is precisely to partition the overall enthalpy

change of a reaction into the time frame in which it takes place and to assign relaxation times to the enthalpic components of the reaction.

The nature of the response function measured by a multifrequency calorimeter can be intuitively understood by considering a macromolecular system at the equilibrium midpoint between two states A and B ($A \rightleftharpoons B$). Under those conditions one imposes on the system a temperature oscillation that shifts the equilibrium alternatively to the left and right of the reaction. Simultaneously, the amount of heat that is absorbed and released as the reaction shifts to the right and left is measured. If the frequency of the excitation temperature oscillation is sufficiently slow when compared to the relaxation time of the reaction, then the macromolecular system will essentially "follow" the wave. On the other hand, at faster excitation frequencies the macromolecular system will be progressively unable to follow the temperature oscillation, and the amount of heat absorbed or released will diminish.

In a multifrequency calorimetry experiment, the amplitude (or phase shift) of the temperature oscillations on the response side of the sample compartment are compared to those that would have been observed if there were not a transition as a function both of temperature and frequency. The fundamental quantity of interest is the ratio of the response amplitude in the absence of a transition (A°) to that in the presence of a transition (A). For the case of multiple independent transitions this quantity is given by the following equation:

$$A^\circ/A = \exp \left[x(vB/C_p^\circ)^{1/2} \sum \frac{C_{pj}^{\text{ex}}(1 + 2\pi v\tau_j)}{1 + (2\pi v\tau_j)^2} \right] \quad (11)$$

where x is the cell thickness, C_p° is the bulk heat capacity of the solution, C_{pj}^{ex} is the excess heat capacity associated with the j th transition, and τ_j the relaxation time associated with that transition. Equation (11) can be analyzed by a nonlinear least-squares fitting algorithm to give the relaxation times and their corresponding contributions to the thermodynamic excess heat capacity function. In Eq. (11), B includes all the constant terms including the instrument calibration constant.^{34a}

The quantity A°/A has very important features, as demonstrated for the case of a single relaxation process. In this case, the temperature-frequency surface defined by A°/A has a maximum located at a temperature equal to T_m and at a frequency equal to $\frac{1}{2}\pi\tau$. This is due to the excess heat capacity being maximal at T_m and the system being excited at its natural frequency. In general, the relaxation modes of the frequency-dependent heat capacity are characterized by the amplitudes, C_{pj}^{ex} , and the relaxation times, τ_j , characteristic of the folding-unfolding transition. Figure 9 shows a com-

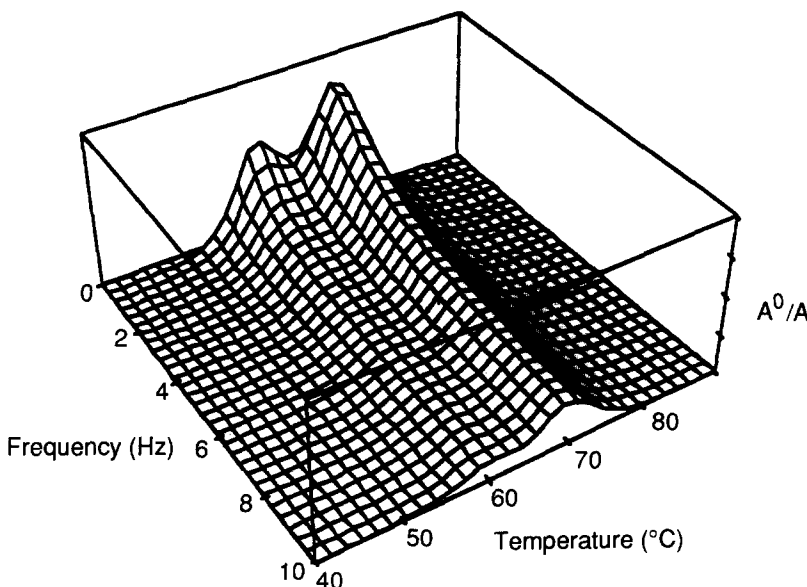


FIG. 9. Computer-simulated temperature and frequency dependence of the normalized multifrequency calorimetry response amplitude for a hypothetical transition composed of two peaks characterized by relaxation times of 200 and 500 msec.

puter-simulated response amplitude frequency-temperature surface for the case of two independent transitions characterized by two different relaxation times.

Applications

Multifrequency calorimetry has been applied to the analysis of membrane phase transitions¹¹⁸ and to the folding-unfolding transition of the protein cytochrome *c*.¹²⁰ It is expected that in the years to come it will find an important niche in the field of nucleic acids research. It is well known that nucleic acids produce complex calorimetric unfolding profiles characterized by the presence of multiple components corresponding to different structural regions of the molecule. Multifrequency calorimetry offers an extra dimension to the analysis, and as such it should improve the resolution of complex nucleic acid transitions.

Concluding Remarks

We began this chapter by noting that calorimetry occupies a venerable place in the history of science. We conclude with the hope that the contents of this chapter have demonstrated calorimetry to be a powerful tool in

biophysical research, capable of uniquely providing thermodynamic and extrathermodynamic characterizations of DNA structure, conformational transitions, and ligand interactions. It should be appreciated that the calorimetric techniques described here are general and therefore also can be applied to the study of other biopolymer systems and their interactions. Only recently, however, has the scientific community begun to appreciate the impressive information content of calorimetric techniques. We hope this chapter serves to advertise the full potential of calorimetry as a powerful experimental tool in the arsenal of techniques available to biophysical chemists.

Acknowledgments

This work was supported by grants from the National Institutes of Health: GM23509 (K.J.B.), GM34469 (K.J.B.), CA47795 (K.J.B.), RR04328 (E.F.), NS24520 (E.F.), and GM37911 (E.F.).